

Section 9

**Development of and studies with
coupled ocean-atmosphere models**

Verification of the new JMA's EPS for Long Range Forecasting based on SVS-LRF

Kohshiro Dehara¹, Hirotohi Mori¹, Masayuki Hirai¹, Noriyuki Adachi¹

¹ Climate Prediction Division, Japan Meteorological Agency, Tokyo, Japan
(E-mail: dehara@met.kishou.go.jp)

1. Introduction

The ensemble prediction system (EPS) for long range forecasting of JMA was replaced. This update is fundamental, because an atmospheric global circulation model (AGCM) is abandoned as a long range forecasting model and an atmosphere-ocean coupled global circulation model (CGCM) is introduced. The operational information of the seasonal prediction has been produced with the new system since February 2010.

We carried out the hindcast experiment based on the standardized verification system for long range forecasts (SVS-LRF; WMO 2006). This paper reports prediction skill of the new system comparing with the old one.

2. Design of the hindcast experiment

Table 1 shows specifications of the hindcast experiment. The major changes of the prediction system between the new system (CGCM) and the conventional one (AGCM) are as follows

* The forecasting model is replaced from AGCM to CGCM, although the atmospheric component of CGCM is basically same as AGCM.

* Ensemble method is changed. CGCM adopts the combination of initial perturbation method and the lagged average forecasting (LAF) method, while AGCM treats only initial perturbations.

Verification data are referred to COBE-SST (Ishii et al. 2005) for SSTs, JRA-25/JCDAS (Onogi et al. 2007) for atmosphere, and GPCP (Adler et al. 2003) for precipitations.

3. Verification results

(1) Prediction skill of Sea surface temperatures

Prediction skill of CGCM is compared with the persistence forecasting (PERSISTENCE). Figure 1 shows anomaly correlation coefficient (ACC) of NINO3.4SSTs (170°E-120°W, 5°S-5°N). A remarkable persistency barrier is found in spring. In contrast, ACC of CGCM is much higher than that of PERSISTENCE. However, prediction skill is relatively insufficient from spring to summer as the other numerical and statistical models (Jin et al. 2008).

(2) Prediction skill of atmosphere

Prediction skill of atmosphere for summer (JJA) with the initial month of February is compared. Figure

2 shows the reliability diagrams of sea-level pressure at tropics (20°S-20°N) for upper tercile events. Reliability of CGCM is nearer the diagonal, so it is better than that of AGCM. Brier Skill Score (BSS) of CGCM is larger than that of AGCM. ACC of stream function at 850hPa of CGCM is larger than that of AGCM in large parts of the Pacific, especially from Southeast Asia to the northwest part of the Pacific and in the northeast part of the Pacific. This indicates that CGCM improves prediction skill of large scale atmospheric circulations in the tropics. This may relate to refinement of prediction of tropical precipitation. CGCM improves prediction skill of precipitation over the Western North Pacific Monsoon (WNPM) region (10°N-20°N, 110°E-160°E) (Figure 4). The cause of this may be that air-sea interaction, such as negative correlation between SSTs anomaly and precipitation in the WNPM region, is considered properly by CGCM comparing with AGCM.

References

- Adler, R.F., G.J. Huffman, A. Chang, R. Ferraro, P. Xie, J. Janowiak, B. Rudolf, U. Schneider, S. Curtis, D. Bolvin, A. Gruber, J. Susskind, P. Arkin, E. Nelkin, 2003: The Version 2 Global Precipitation Climatology Project (GPCP) Monthly Precipitation Analysis (1979-Present). *J. Hydrometeor.*, **4**, 1147-1167.
- Ishii, M., A. Shouji, S. Sugimoto, and T. Matsumoto, 2005: Objective Analyses of Sea-Surface Temperature and Marine Meteorological Variables for the 20th Century using ICOADS and the Kobe Collection. *Int. J. Climatol.*, **25**, 865-879.
- Jin E. K., James L. Kinter III, B. Wang, C.-K. Park, I.-S. Kang, B. P. Kirtman, J.-S. Kug, A. Kumar, J.-J. Luo, J. Schemm, J. Shukla and T. Yamagata, 2008: Current status of ENSO prediction skill in coupled ocean-atmosphere
- Onogi, K., J. Tsutsui, H. Koide, M. Sakamoto, S. Kobayashi, H. Hatsushika, T. Matsumoto, N. Yamazaki, H. Kamahori, K. Takahashi, S. Kadokura, K. Wada, K. Kato, R. Oyama, T. Ose, N. Mannoji, and R. Taira, 2007: The JRA-25 Reanalysis. *J. Meteor. Soc. Japan*, **85**, 369-432.
- WMO, 2006: Standardised Verification System (SVS) for Long-Range Forecasts (LRF), New Attachment II-8 to the Manual on the GDPFS (WMO-No. 485), Volume I, 28pp.

Table 1 Specifications of the conventional and the new system for long range forecasting

		Old system (AGCM)	New system (CGCM)
Outline of the system		AGCM with two-tier method	CGCM (one-tier method + flux adjustment)
Model	Atmospheric component	JMA-GSM (TL95 (~1.125°), 40 levels (up to 0.4 hPa))	
	Oceanic component	---	MRI.COM (1.0° in longitude, 0.3°~1.0° in latitude, up to 50 levels, 75°N-75°S)
Initial condition	Atmosphere	JRA-25/JCDAS	
	Ocean	---	MOVE/MRI.COM-G
Boundary condition	Land surface	numerical prediction initialized from climatology	
	SST	two-tiered method (persisted anomaly + statistical prediction)	numerical prediction with flux adjustment climatology out of the oceanic model domain (polar region)
	Sea ice	climatology	
Parameter	CO ₂	constant	trend
Ensemble method	Ensemble size	11	10 (5 BGMs and 15-day LAF)
	Perturbation method	singular vector (SV) method	combination of initial perturbation (atmospheric breeding growing mode (BGM) method and oceanic initial perturbation) and lagged average forecast (LAF) method
Hindcast	Target period	1984~2005	1979~2008
	Initial dates	10th of the every month	the beginning of month and the middle of the preceding month

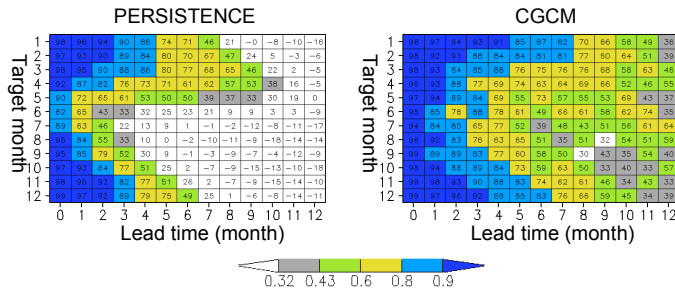


Figure 1 Anomaly correlation coefficient (ACC) of NINO.3.4 (170°E-120°W, 5°S-5°N) SSTs during 1979-2007 with respect to target month (vertical) and leadtime (horizontal) by persistence (left) and CGCM (right). The two-digit number denotes 100 times ACC. 0.32 and 0.43 of ACC are equivalent to 5% and 1% significant level of one-side t-test, respectively.

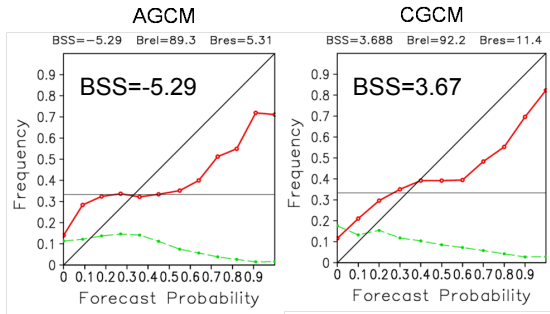


Figure 2 Reliability Diagrams of sea-level pressure for summer (JJA) with the initial month of February at tropics (20°S-20°N) for upper tercile events. Full(Red) : Reliability, Dash(green) : Forecast Frequency, BSS: Brier Skill Scores x 100

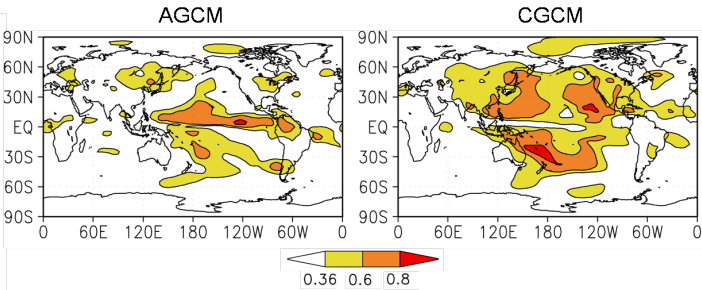
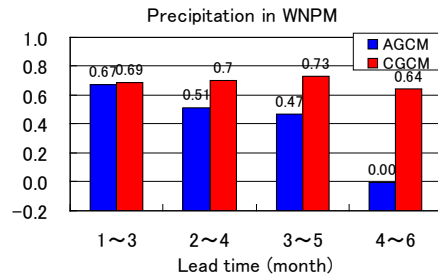


Figure 3 Anomaly correlation coefficient of stream function at 850hPa for summer (JJA) with the initial month of February by AGCM (left) and CGCM (right). Target period is 1984~2005. 0.36 of ACC is equivalent to 5% significant level of one-side t-test.

Figure 4 Anomaly correlation coefficient of 3-month mean of precipitation for summer (JJA) with the initial month of February over Western North Pacific Monsoon region (110°E-160°E, 10°N-20°N) with respect to lead time by AGCM (Blue) and CGCM (Red). Target period is 1984~2005.



Replacement of the JMA's EPS for Long Range Forecasting in February 2010

Masayuki Hirai¹, Ichiro Ishikawa¹, Akihiko Shimpo¹, Hitoshi Sato¹, Taizo Soga¹, Hirotohi Mori¹,
Noriyuki Adachi¹, Yosuke Fujii², Satoshi Matsumoto² and Tamaki Yasuda³

¹Climate Prediction Division, Japan Meteorological Agency, Tokyo, Japan

²Oceanographic Research Department, Meteorological Research Institute, Tsukuba, Japan

³Climate Research Department, Meteorological Research Institute, Tsukuba, Japan

(E-mail: m-hirai @ met.kishou.go.jp)

1. Introduction

The ensemble prediction system (EPS) for long range forecasting in Japan Meteorological Agency (JMA) was replaced. The old system employed a two-tier method, in which an atmospheric global circulation model (AGCM) was executed using the prescribed SSTs obtained by a combination of persisted SST anomalies in the preceding month and statistically derived ones based on the ENSO prediction with the coupled ocean-atmosphere general circulation model (CGCM) operated for JMA's El Niño prediction. The new system employs a one-tier method using the CGCM. The CGCM is based on the one used as the El Niño prediction system. Accordingly, the new system is used for both long range forecasting and the El Niño outlook. The operational information of the seasonal prediction and the El Niño outlook has been produced with the new system since February and March 2010, respectively. This paper reports the outline of the new system.

2. Major changes in this update

Table 1 shows the specifications of the old and the new system. The major changes are as follows.

(1) Change from AGCM to CGCM (Figure 1)

The forecasting model is changed from the AGCM to the CGCM. The atmospheric part of the CGCM is basically same as the AGCM, which is a low-resolution version of the JMA's AGCM for short- and medium-range forecasting. The oceanic part of the model is called MRI.COM (Tsujino et al. 2010)¹, which has been developed at the Meteorological Research Institute/JMA.

The coupling between the ocean and the atmosphere is performed every hour. The atmospheric component supplies hourly-mean heat, momentum and freshwater fluxes to the ocean component, while the oceanic component supplies the SSTs to the atmospheric component. Simulated fields in the CGCM tend to approach the model climate state, which differs substantially from the real states. In order to suppress this climate drift, adjustment is made to both the heat and momentum fluxes. The adjustment amount is the statistics depending on a target month.

¹http://www.mri-jma.go.jp/Publish/Technical/DATA/VOL_59/59.h tml

(2) Initial conditions and perturbations

Initial conditions for atmosphere are obtained from the result of analysis by the JMA Climate Data Assimilation System (JCDAS; Onogi et al. 2007), which is a quasi-real-time climatic assimilation system under the same conditions as that for JRA-25. Initial conditions for ocean are obtained from the global ocean data assimilation system (MOVE/MRI.COM-G; Usui et al. 2006).

In the new system, initial perturbations for both atmosphere and ocean are generated. Atmospheric initial perturbations are obtained using the Breeding of Growing Modes (BGM) method, estimating for the Northern Hemisphere (20°N-90°N) and the tropics (20°S-20°N) separately. Oceanic initial perturbations are obtained through MOVE/MRI.COM-G, in which perturbed surface heat and momentum fluxes in the tropics adopted.

(3) Ensemble method

The new system adopts a combination of the initial perturbation method and the Lagged Average Forecasting (LAF) method. The purposes of adoption of the LAF method are to avoid the intensive use of computing resources and to ensure ensemble spread in ocean. According to the hindcast experiment, ensemble spread in ocean is underestimated if the LAF method is not adopted. Nine members are run every five days, and the EPS consists of fifty-one members for the latest six initial dates (Figure 2).

References

- Onogi, K., J. Tsutsui, H. Koide, M. Sakamoto, S. Kobayashi, H. Hatsushika, T. Matsumoto, N. Yamazaki, H. Kamahori, K. Takahashi, S. Kadokura, K. Wada, K. Kato, R. Oyama, T. Ose, N. Mannoji, and R. Taira, 2007: The JRA-25 Reanalysis. *J. Meteor. Soc. Japan*, **85**, 369-432.
- Tsujino, H., T. Motoi, I. Ishikawa, M. Hirabara, H. Nakano, G. Yamanaka, T. Yasuda, and H. Ishizaki, 2010: Reference manual for the meteorological research institute community ocean model (MRI.COM) version 3. *Technical Reports of the Meteorological Research Institute*, **59**, 241pp.
- Usui, N., S. Ishizaki, Y. Fujii, H. Tsujino, T. Yasuda and M. Kamachi, 2006: Meteorological Research Institute multivariate ocean variational estimation (MOVE) system. *Advances in Space Research*, **37**, 806-822.

Table 1 Specifications of the old and the new system for long range forecasting in JMA

Outline of the system		Old system (AGCM)	New system (CGCM) (from Feb. 2010)
Model	Atmospheric component	JMA-GSM (TL95 (~1.125°), 40 levels (up to 0.4 hPa))	
	Oceanic component	---	MRI.COM (1.0° in longitude, 0.3°-1.0° in latitude, 50 levels, 75°N-75°S)
Initial condition	Atmosphere	JMA's global analysis**	JCDAS
	Ocean	---	MOVE/MRI.COM-G
Boundary condition	Land surface	numerical prediction initialized from climatology	
	SST	two-tier method (persisted anomaly + statistical prediction)	numerical prediction with flux adjustment, climatology out of the oceanic model domain (polar region)
	Sea ice	climatology	
Parameter	CO ₂	constant	trend*
Ensemble method	Ensemble size	51	51 (9 BGM and 6 initial days with 5-day LAF)*
	Perturbation method	singular vector (SV) method	combination of initial perturbation (atmospheric breeding growing mode (BGM) method and oceanic initial perturbation) and lagged average forecast (LAF) method

* Specification of the old El Niño prediction system operated until January 2010 is similar to the new system (right), except the items marked by '*'. In the old El Niño prediction system, CO₂ concentration was regarded as constant and ensemble size was 30 (5 BGM and 6 initial days with 5-day LAF).

** Operational atmospheric data assimilation system for a short-range forecasting in JMA.

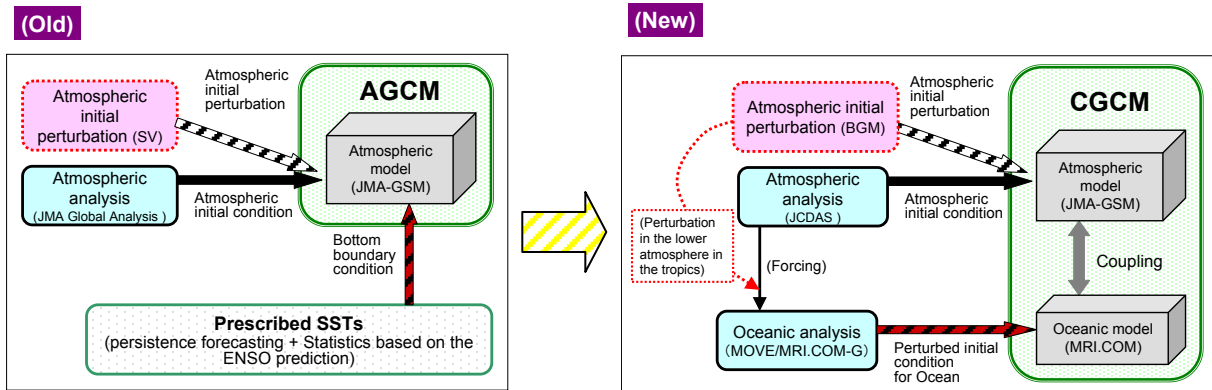


Figure 1 Schema of the old (left) and new (right) prediction system for long range forecasting
The green, aqua and red boxed processes denote the forecasting model, the data assimilation and the initial perturbation, respectively.

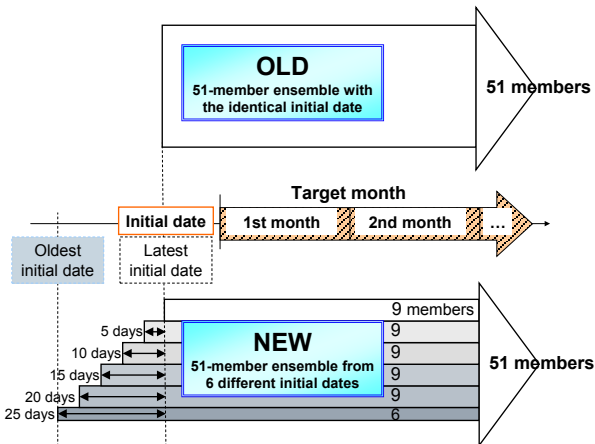


Figure 2 Schema of aggregation for the ensemble members in the old (top) and new (bottom) ensemble prediction system for long range forecasting.

Recent Developments in MRD coupled Atmosphere-Ocean-Ice Modelling

*Hal Ritchie, Meteorological Research Division, EC, Dartmouth NS,
Christiane Beaudoin, Meteorological Research Division, EC, Dorval QC
Jean-Marc Bélanger, Meteorological Research Division, EC, Dorval QC
Serge Desjardins, Meteorological Service of Canada, EC, Dartmouth NS
Manon Faucher, Canadian Meteorological Centre, EC, Dorval QC
Roop Lalbeharry, Meteorological Research Division, EC, Downsview ON
Syd Peel, Meteorological Research Division, EC, Downsview ON
Pierre Pellerin, Meteorological Research Division, EC, Dorval QC
Sanjay Rattan, Meteorological Research Division, EC, Downsview ON
François Roy, Canadian Meteorological Centre, EC, Dorval QC
Greg Smith, Meteorological Research Division, EC, Dorval QC

Coupled numerical environmental prediction research is pivotal to meeting Environment Canada's key priority for integrated environmental monitoring and prediction. Our focus is on developing coupled atmosphere-ocean-ice modelling systems in order to improve the accuracy of environmental forecasts on time scales from minutes to seasons and space scales from kilometres to global. Progress in both deterministic and ensemble environmental forecast systems is crucial for applications such as managing hydrological, energy, land and marine resources, and preparedness for environmental emergencies. This is being accomplished by contributing to and leveraging research, information and data through national and international partnerships. One notable example is the Canadian Operational Network of Coupled Environmental Prediction Systems (CONCEPTS) in which Environment Canada (EC), Fisheries and Oceans Canada (DFO) and the Department of National Defence (DND) are developing atmosphere-ocean-ice systems in partnership with Mercator-Océan (France) for ocean aspects based on their Nucleus for European Modelling of the Ocean (NEMO) system, and with the university Global Ocean-Atmosphere Prediction and Predictability (GOAPP) research network funded by the Canadian Foundation for Climate and Atmospheric Sciences (CFCAS). CONCEPTS is providing a framework for research and operations that will provide environmental information products and capabilities required by EC, DFO and DND.

EC's Meteorological Research Division (MRD) has made considerable progress on the installation of the existing 1/4-degree Mercator ocean data assimilation and prediction system at the Canadian Meteorological Centre (CMC). The NEMO model configuration has been installed and validated by comparing with Mercator forecasts using initial conditions and forcings provided by Mercator for a 2-week period. Subsequently the NEMO model, initiated by Mercator analyses, is being driven by the operational CMC GEM atmospheric model forcings to potentially produce a 2-member ensemble together with Mercator forecasts. Installation of the Mercator SAM2 Ocean

* *Corresponding author address:* Harold Ritchie, Environment Canada, 45 Alderney Drive, Dartmouth NS, Canada B2Y 2N6; E-mail: Harold.Ritchie@ec.gc.ca

Data Assimilation system has been validated by reproducing Mercator analyses using the same input data, initial conditions, and forcings. Initial coupling of 1 degree global NEMO and GEM forecast models has also been completed, and coupling of ¼ degree NEMO and meso-global GEM forecast models is in progress.

Our most advanced project is the fully interactive coupled atmosphere-ocean-ice forecasting system for the Gulf of St. Lawrence (GSL) that has been installed in experimental mode at CMC. This project follows a study by Pellerin et al. (2004) showing more accurate weather forecasts over the GSL and adjacent coastal areas resulting from the coupled system in a case study involving rapid ice motion. This has been confirmed in more extensive testing and preparations for operational use that were carried out in a collaboration amongst several groups in EC and DFO. Results during the past year have demonstrated that the coupled system produces improved forecasts in and around the GSL during all seasons, proving that atmosphere-ocean-ice interactions are indeed important even for short-term Canadian weather forecasts. This has important implications for CONCEPTS and other coupled modeling and data assimilation partnerships that are in progress. It is anticipated that this GSL system will soon become the first fully interactive coupled system to be implemented at CMC.

Within our coupled modelling activity there is also a particular focus on sea ice in order to improve its representation in models used for forecasting of weather, climate and sea-ice features. An offline atmosphere-ice modelling system has been developed and is being used to produce ice forecasts over various Canadian regions and is being incorporated in sea ice data assimilation cycles.

Another activity focuses on wave modeling and ensembles. A project entitled “An ensemble modeling system for winds and waves” has been highly successful in keeping Canada’s wave model competitive with wave models in other countries, and has allowed the Canadian model to take advantage of improvements in data assimilation and in atmospheric modeling, thus providing optimal environmental information, predictions and services to ensure safety and support economic activity for which waves are an important consideration. Another project on “Development of Probabilistic Forecast Tools for Search and Rescue” is carrying out research and development aimed at enhancing the marine weather and wave forecast information that is made available to Search and Rescue for predicting target location, and to improve the forecast information available to all marine interests for high impact weather events. The goal is to quantify the uncertainty in forecasts of important marine elements such as winds and waves, so that forecast products can be presented in terms of probabilities of occurrence of important weather events, in addition to the current practice of specifying the expected location and time of the occurrence of a significant event. Such probability estimates of wind, for example, can then be used as input to models such as CANSARP (CANadian Search And Rescue Planning) and the wave model (WAM), to give probabilities of target location in the former case and probabilities of high wave heights in the latter case.

Reference

Pellerin, P., H. Ritchie, F.J. Saucier, F. Roy, S. Desjardins, M. Valin and V. Lee, 2004 : Impact of a two-way coupling between an Atmospheric and an ocean-ice model over the Gulf of St. Lawrence. *Mon. Wea. Rev.*, 132, 1379-1398.

Impacts of diurnally-varying sea-surface temperature on the predictions of Typhoon Hai-Tang in 2005. Part I. Intensity prediction.

Akiyoshi Wada^{1*}, Yoshimi Kawai² and Norihisa Usui¹

- 1) Meteorological Research Institute, Tsukuba, Ibaraki, 305-0052, JAPAN
 2) Japan Agency for Marine-Earth Science and Technology, Yokosuka, Kanagawa, 237-0061, JAPAN.

1. Introduction

Wada and Kawai [2009a, 2009b] described the formulation on the basis of Schiller and Godfrey [2005] and Ohlmann and Siegel [2000] for calculating skin temperature in the ocean and showed the results of 1-D numerical experiments using an atmosphere-ocean coupled model. The impact of diurnally-varying sea-surface temperature (SST) on the atmosphere was relatively small and interestingly wind stress increases on alternative days. In the present study, we extend the scheme for the prediction of Typhoon Hai-Tang in 2005. We investigate the impacts of diurnally-varying SST on Hai-Tang's predictions using both the nonhydrostatic model (NHM) and the NHM coupled with a mixed-layer ocean model (NCM). We perform the numerical experiments for checking the sensitivity of skin temperature to TC intensity predictions. In the Part I, we focus on whether or not the impact of diurnally-varying SST is distinguished from the impact of random noise.

2. Experiment Design

The specification of numerical-prediction experiments is as follows. The NHM and NCM have 721 x 421 horizontal grids with a horizontal grid spacing of 6km, 40 vertical levels with variable and stretch intervals from 40m at the lowermost layer near the surface to 1180m at the uppermost layer and the top height of nearly 23km.

Oceanic initial conditions are obtained from daily oceanic reanalysis data with a horizontal resolution of 0.5° calculated by the Meteorological Research Institute Ocean Variational Estimation system [Usui et. al. 2006]. Oceanic reanalysis data used in the present study is daily output in 1999 and 2005.

Table 1 lists numerical-prediction experiments in the present study. Here, the abbreviation 'SG' indicates the experiments by the coupled atmosphere-ocean model with a diurnally-varying SST scheme, the abbreviation 'NO' indicates the experiments by the coupled atmosphere-ocean model without a diurnally-varying SST scheme, and the abbreviation 'NH' indicates the experiments by the atmosphere model.

Uniform random real numbers in the interval (0,0.1] are generated using the multiplicative congruence method. In experiments A, B, and C, the random numbers are added instead of the skin temperature overall the computational domain, while the random numbers are added instead of the skin temperature where the amplitude of skin temperature is higher than 0.1°C in experiments D, E, F. The random numbers are regarded as random noises in this study.

To validate the results of numerical-prediction experiments, best-track positions and central pressures archived by the Regional Specialized Meteorological Center are used. In the present study, central pressures are regarded as a reference of Hai-Tang's intensity.

Table 1 Abbreviations of Numerical-Prediction Experiments, Year of Oceanic Precondition, and Coupled / Noncoupled Ocean Model with (SG) or without (NO) an oceanic sublayer scheme or Noise Patterns and its Areas

EXP.	YEAR	SG/NO/NOISE & Couple/Noncouple
SG05	2005	SG & Couple
NO05	2005	NO & Couple
NH05	2005	NO & Noncouple
NEA05	2005	NOISE (+0~0.1 overall the area) & Couple
NEB05	2005	NOISE (-0.05~0.05 overall the area) &
NEC05	2005	NOISE (-0.1~0 overall the area) & Couple
NED05	2005	NOISE (+0~0.1 where diurnal amplitude >
NEE05	2005	NOISE (-0.05~0.05 where diurnal
NEF05	2005	NOISE (-0.1~0 where diurnal amplitude >
SG99	1999	SG & Couple
NO99	1999	NO & Couple
NH99	1999	NO & Noncouple
NEA99	1999	NOISE (+0~0.1 overall the area) & Couple
NEB99	1999	NOISE (-0.05~0.05 overall the area) &
NEC99	1999	NOISE (-0.1~0 overall the area) & Couple
NED99	1999	NOISE (+0~0.1 where diurnal amplitude >
NEE99	1999	NOISE (-0.05~0.05 where diurnal
NEF99	1999	NOISE (-0.1~0 where diurnal amplitude >

Table 2 Diurnal Amplitude of Sea-Surface Temperature Calculated in the domain around 10-30°N, 120-160°E.

	0-24h (°C)	25-48h (°C)	49-72h (°C)
SG05	1.39	3.07	0.82
NO05	0.71	0.60	0.51
SG99	2.64	3.82	1.49
NO99	0.63	0.59	0.65

3. Results

Table 2 shows the amplitude of diurnally-varying SST every 24h. The amplitude of diurnally-varying SST is notable from 25h to 48h. Figure 1 displays horizontal distributions of the amplitude of diurnally-varying SST from 25h to 48h when the amplitude is notable (Table 2). The amplitude of diurnally-varying SST is close to zero around Hai-Tang and is relatively low along Hai-Tang's track. In contrast, the amplitude of diurnally-varying SST is relatively high where the area is far from Hai-Tang's track. The effect of new scheme for calculating the skin temperature is remarkable around the area. This indicates that new scheme hardly affect the calculation of sea-surface cooling induced by Hai-Tang.

Figure 2 depicts the time series of predicted central pressures listed in Table 1. All predicted central pressures are higher than best-track central pressures after 24h. A difference in predicted central pressures between Fig. 2a and Fig. 2b indicates that predicted central pressures are influenced by oceanic precondition, not diurnally-varying SST and random noises. There seems to be no difference between random noises overall the domain and over the limited domain where the amplitude of diurnally-varying SST is higher than 0.1 °C.

However, the impact of random noises overall the domain on central pressure prediction is less than 1 hPa from 6h to 24h (Fig. 2c). The random noises around Hai-Tang's track directly affect central pressure prediction. Figure 2c indicates that we cannot distinguish the impacts of diurnally-varying SST on central pressure prediction from those of the random noises even though a difference between SG and NO becomes salient at certain integration times. The impact of diurnally-varying SST and the random noises far from Hai-Tang's track on central pressure prediction is significant after 24h in the present study.

References

Ohlmann, J.C., and D.A. Siegel, 2000: Ocean Radiant Heating. Part II: Parameterizing Solar Radiation Transmission through the Upper Ocean. *J. Phys. Oceanogr.*, 30, 1849–1865.

Schiller, A., and J. S. Godfrey, 2005: A diagnostic model of the diurnal cycle of sea surface temperature for use in coupled ocean-atmosphere models. *J. Geophys. Res.*, 110, C11014, doi:10.1029/2005JC002975.

Usui, N., S. Ishizaki, Y. Fujii, H. Tsujino, T. Yasuda and M. Kamachi, 2006: Meteorological Research Institute multivariate ocean variational estimation (MOVE) system: Some early results. *J. Adv. Space Res.*, 37, 806-822.

Wada, A., and Y. Kawai, 2009a: The development of diurnally-varying sea-surface temperature scheme. Part I. Preliminary numerical experiments. CAS/JSC WGNRE Research Activities in Atmosphere and Oceanic Modelling, 0907-0908.

Wada, A., and Y. Kawai, 2009b: The development of diurnally-varying sea-surface temperature scheme. Part II. Idealized numerical experiments. CAS/JSC WGNRE Research Activities in Atmosphere and Oceanic Modelling, 0909-0910.

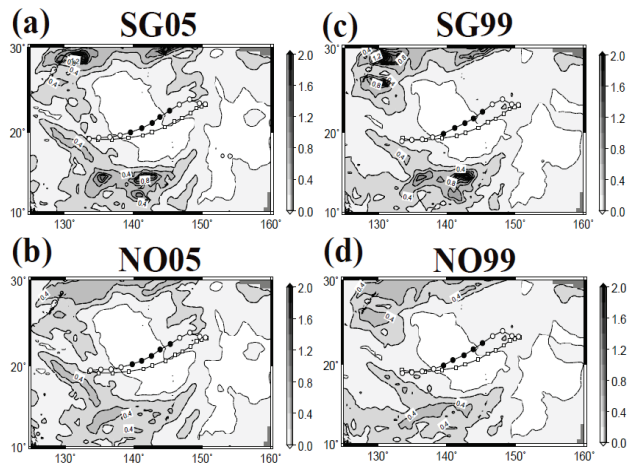


Fig.1 Horizontal distribution of the amplitude of diurnally-varying SST (°C) from 25h to 48h in (a) SG05, (b) NO05, (c) SG99, and (d) NO99.

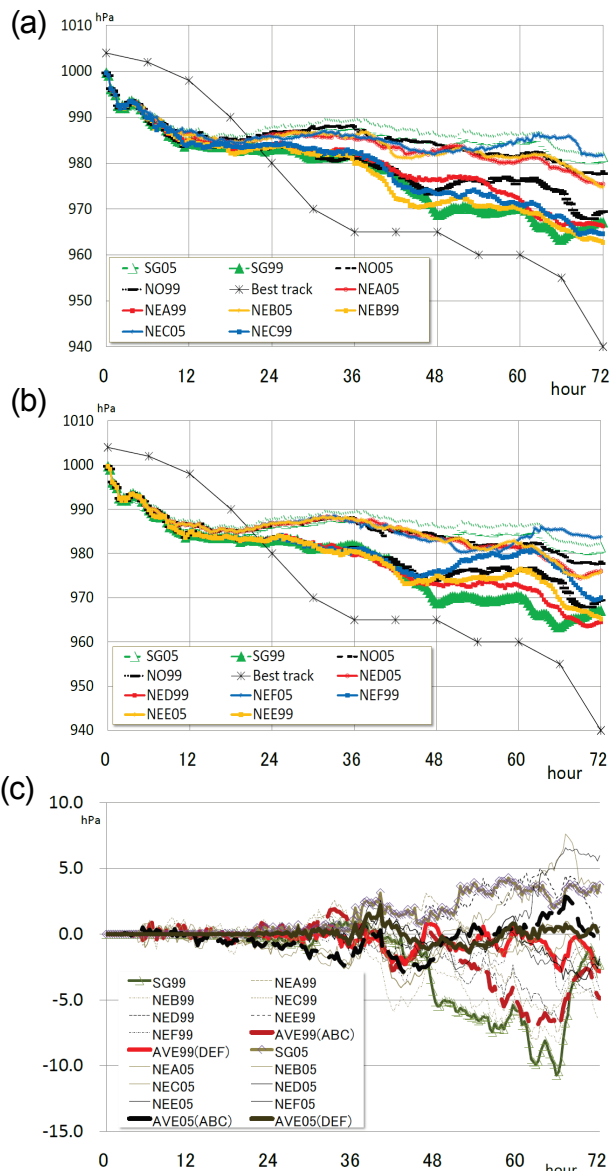


Fig.2 Time series of predicted central pressure in (a) experiments A, B, and C, (b) experiments D, E, and F, and (c) deviations from SG to NO and their averages.

This work was supported by Japan Society for the Promotion of Science (JSPS), Grant-in-Aid for Scientific Research (C) (19612005).

Impacts of diurnally-varying sea-surface temperature on the predictions of Typhoon Hai-Tang in 2005.

Part II. The impact on the thermodynamics field around Hai-Tang's center.

Akiyoshi Wada ^{1*}, Yoshimi Kawai² and Norihisa Usui¹

- 1) Meteorological Research Institute, Tsukuba, Ibaraki, 305-0052, JAPAN
- 2) Japan Agency for Marine-Earth Science and Technology, Yokosuka, Kanagawa, 237-0061, JAPAN.

1. Introduction

Wada et al. [2010] reported that the impacts of diurnally-varying sea-surface temperature (SST) on central pressure prediction could not be distinguished from those of the random noises in the case of the numerical prediction of Typhoon Hai-Tang in 2005 using the nonhydrostatic model (NHM) and the NHM coupled with a mixed-layer ocean model (NCM). However, the impacts of diurnally-varying SST might be significant on Hai-Tang's thermodynamics field such as the distribution of hourly precipitation even though the impact of diurnally-varying SST on central pressures and maximum wind speeds could be regarded as that of random noises. This paper investigates the impact of diurnally-varying SST on thermodynamics fields such as specific humidity within a radius of 300km, liquid water (specific cloud plus specific rain) within a radius of 300km from the surface to nearly 6.5km, and an hourly trend of temperature due to radiation within a radius of 300km from nearly 6.5km to nearly 14km, regarded as a warm-core temperature trend.

2. Methods

The specification of numerical experiments for Hai-Tang's predictions is as follows. The NHM and NCM have 721 x 421 horizontal grids with a horizontal grid spacing of 6km, 40 vertical levels with variable and stretch intervals from 40m at the lowermost layer near the surface to 1180m at the uppermost layer, and the top height of nearly 23km.

A series of numerical experiments is listed in Table 1. The experiment design was described in Wada et al. [2010]. On the basis of the results of Hai-Tang's predictions, we determine the horizontal area within a radius of 300km from Hai-Tang's center determined by minimum sea-surface pressure. The ranges of layers vertically averaged are from the lowermost layer to 32 (nearly 14km) in specific humidity, from the lowermost layer to 22 (nearly 6.5km) in liquid water, and from 22 to 32 in hourly trend of temperature due to radiation.

We investigate the average of the deviations from the central pressures in seven experiments (SG05, NEA05-NEF05) to the central pressures in NO05 and their standard deviations. If the average in SG05 ranges within the standard deviations, the impact of diurnally-varying SST on the intensity prediction is regarded as the impact of randoms noise on a weather-forecasting scale. Here we show the result of numerical experiments when the oceanic initial condition in 2005 is used.

Table 1 Abbreviations of Numerical-Prediction Experiments, Year of Oceanic Precondition, and Coupled / Noncoupled Ocean Model with (SG) or without (NO) an oceanic sublayer scheme or Noise Patterns and its Areas

EXP.	YEAR	SG/NO/NOISE & Couple/Noncouple
SG05	2005	SG & Couple
NO05	2005	NO & Couple
NH05	2005	NO & Noncouple
NEA05	2005	NOISE (+0~0.1 overall the area)& Couple
NEB05	2005	NOISE(-0.05~-0.05 overall the area) & Couple
NEC05	2005	NOISE(-0.1~0 overall the area) & Couple
NED05	2005	NOISE(+0~0.1 where diurnal amplitude > 0.1)
NEE05	2005	NOISE(-0.05~-0.05 where diurnal amplitude >
NEF05	2005	NOISE(-0.1~0 where diurnal amplitude > 0.1)

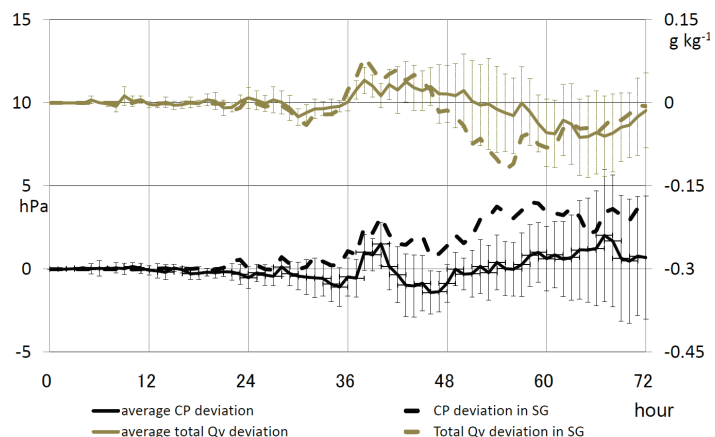


Fig.1 Solid lines indicate the averages of central pressure (black) and specific humidity (gray). Dashed lines indicate the results of central pressure (black) and specific humidity (gray) in SG05.

3. Results

Figure 1 depicts the evolution of the average of the deviations of central pressure and specific humidity from that in NO05 among seven numerical experiments except for NO05 and the evolution of the deviations of central pressure and specific humidity between SG05 and NO05. Central pressure in SG05 tends to be higher than that in NO05. However, the deviation exceeds the standard deviation only from 36h to 60h when the amplitude of diurnally-varying SST is high [Wada et al., 2010]. During the period, the specific humidity in SG05 is higher than the average value around 38h and turns to be lower than the average value around 56h. After the change in the trend of specific humidity around 46h, the impact of diurnally-varying SST on central pressure prediction in SG05 becomes significant and continues until 62h.

Figure 2 depicts the evolution of the average of the deviations of central pressure and liquid water from that in NO05 among seven numerical experiments except for NO05 and the evolution of the deviations of central pressure and liquid water between SG05 and NO05. During the period, the liquid water in SG05 is significantly lower than the average value around 38h and turns to be higher than the average value from 42h to 56h. A decrease in liquid water precedes an increase in specific humidity.

Figure 3 depicts the evolution of the average of the deviation of hourly trend of temperature due to radiation from that in NO05 among seven numerical experiments except for NO05 and the evolution of the deviation of hourly trend of temperature due to radiation between SG05 and NO05. The deviations are significant after 36h when the deviations of specific humidity (Fig. 1) and liquid water (Fig. 2) become salient. However, the deviation exceeds the standard deviation only from 48h to 56h. This implies that the impact of diurnally-varying SST on warm-core temperature trend is only significant from 48h to 56h, probably because of a significantly increase in liquid water. The period from 48h to 56h corresponds to the period shortly after the amplitude of diurnally-varying SST is high ($\sim 3^{\circ}\text{C}$, see Table 2 in Wada et al. [2010]). Differently from the deviations of specific humidity and liquid waters, the amplitude of the deviation of hourly trend of temperature due to radiation between SG05 and NO05 varies on a shorter time scale, implying that the variation is affected not only by diurnally-varying SST but also by atmospheric radiation. This result indicates that the impact of diurnally-varying SST on Hai-Tang's prediction is non-linearly influenced by atmospheric thermodynamics.

4. Concluding remarks

From the sensitivity experiments, we conclude that the impact of diurnally-varying SST on the prediction of Typhoon Hai-Tang in 2005 cannot be distinguished from the impact of a noise for SST when the amplitude of diurnally-varying SST is smaller than 3°C . We need to explore the non-linearly atmospheric-oceanic processes after the impact of diurnally-varying SST on atmospheric ingredients exceeds the standard deviation.

References

Wada, A., Y. Kawai and N. Usui, 2010: Impacts of diurnally-varying sea-surface temperature on the predictions of Typhoon Hai-Tang in 2005. Part II. Intensity prediction. CAS/JSC WGNE Research Activities in Atmosphere and Oceanic Modelling, Submitted.

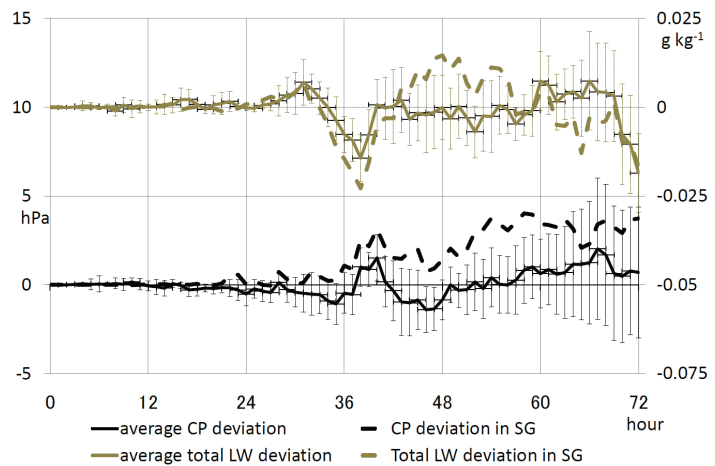


Fig.2 Solid lines indicate the averages of central pressure (black) and liquid water (gray). Dashed lines indicate the results of central pressure (black) and liquid water (gray) in SG05.

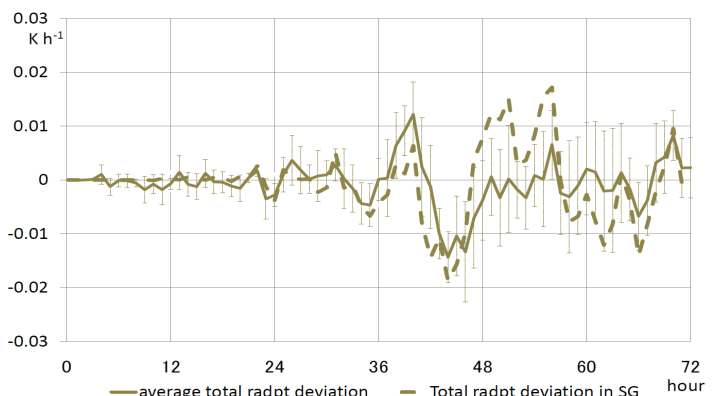


Fig.3 Solid lines indicate the averages of hourly trend of temperature due to radiation. Dashed lines indicate the results of hourly trend of temperature due to radiation in SG05.

This work was supported by Japan Society for the Promotion of Science (JSPS), Grant-in-Aid for Scientific Research (C) (19612005).

The influence of the variation of oceanic precondition on the prediction of Typhoon Hai-Tang in 2005

Akiyoshi Wada and Norihisa Usui

Meteorological Research Institute, Tsukuba, Ibaraki, 305-0052, JAPAN

1. Introduction

Previous results suggest that sea surface cooling (SSC) induced by tropical cyclones (TCs) results in 'negative feedback' for TC intensification [e.g., Wada, 2009]. The ocean response to TCs occurs locally along TC track. In contrast, oceanic environments vary not only on a weather forecasting time scale (for example, above-mentioned SSC) but also on a seasonal to climate time scale (for example El Niño Southern Oscillation). Here, we are interested in how and to what extent the variations of oceanic environment affect TC predictions as pre-existing oceanic conditions, and whether or not the impact is significant. The purpose in the present study is to investigate the influence of the variation of oceanic precondition on the prediction of Typhoon Hai-Tang in 2005 during the intensification phase. We performed numerical-prediction experiments for Typhoon Hai-Tang in 2005 using a coupled atmosphere-ocean model included in an oceanic sublayer scheme for calculating diurnally-varying SST in the upper-ocean skin layer. To investigate the sensitivity of the variation of oceanic precondition to TC predictions, daily oceanic initial conditions on 12 July from 1997 to 2005 and one atmospheric initial and boundary conditions on July in 2005 are specified in this study.

2. Experiment Design

Table 1 shows a list of numerical-prediction experiments. The abbreviation 'SG' indicates numerical-prediction experiments using a coupled atmosphere-ocean model with an oceanic sublayer scheme (hereafter the model is referred to NCM), while the abbreviation 'NH' indicates those using an atmospheric (nonhydrostatic) model (hereafter NHM). In the present study, both NHM and NCM have 721 x 421 horizontal grids with a horizontal grid spacing of 6km, 40 vertical levels with variable intervals from 40m at the lowermost layer near the surface to 1180m at the uppermost layer, and a top height of nearly 23km.

Daily oceanic reanalysis data used for creating oceanic initial conditions are calculated by the Meteorological-Research-Institute Ocean Variational Estimation system [Usui et. al. 2006] with a horizontal grid spacing of 0.5°. Double digits on the left column in Table 1 indicates years from 1997 to 2005 in which daily oceanic reanalysis data on 12 July is used for creating oceanic initial conditions. Therefore, the total number of numerical-prediction experiments is 18.

There are some remarkable oceanic variations on seasonal to climate time scales during the period from 1997 to 2005. The day on 12 July 1999 corresponds to a period when the La Niña event

Table 1 Abbreviations of Numerical-Prediction Experiments, Year of Oceanic Precondition with the El Niño (E) or La Niña (L) Event, and Coupled (SG)/Noncoupled (NH) Ocean

EXPERIMENT	YEAR	SG/NO
SG97	1997(E)	SG
SG98	1998	SG
SG99	1999 (L)	SG
SG00	2000	SG
SG01	2001	SG
SG02	2002(E)	SG
SG03	2003	SG
SG04	2004	SG
SG05	2005	SG
NH97	1997(E)	NO
NH98	1998	NO
NH99	1999(L)	NO
NH00	2000	NO
NH01	2001	NO
NH02	2002(E)	NO
NH03	2003	NO
NH04	2004	NO
NH05	2005	NO

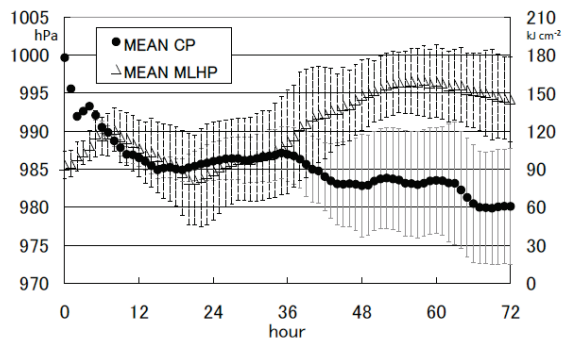


Figure.1 Time series of mean central pressures and mean mixed-layer heat potentials in SG from 1997 to 2005 and their standard deviation.

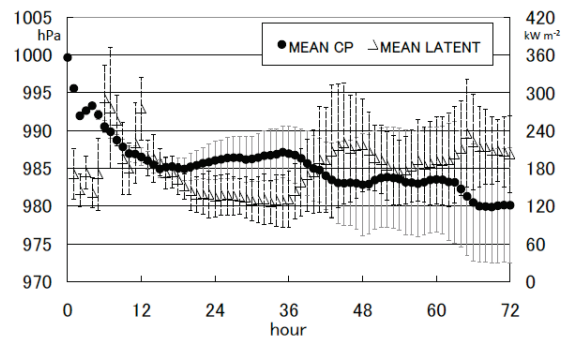


Figure.2 Time series of mean central pressures and mean latent heat fluxes in SG from 1997 to 2005 and their standard deviation.

was mature. In contrast, the day on 12 July 2002 corresponds to a period when the El Niño event was mature. Moreover, the day on 12 July 2005 corresponds to a period when the central Pacific warming event was terminated and it turned to the La Niña event. The year 2004 was a memorable year in the sense that ten typhoons extraordinarily made landfall in Japan.

To validate the results of numerical-prediction experiments, best-track positions and central pressures archived by the Regional Specialized Meteorological Center are used. The best-track data is defined as sustained 10-min mean data. In the present study, predicted central pressure is used as the reference of Hai-Tang's best-track intensity.

3. Results

Figure 1 depicts the time series of mean central pressures (CPs) and mean mixed-layer heat potentials (MLHPs) averaged from 1997 to 2005 in SG and their standard deviations. Mean values are calculated as the average of predicted CPs and MLHPs around predicted Hai-Tang's center. The definition of MLHP was described in Wada [2009]. At the early integration from 0h to 9h, mean CP rapidly falls as mean MLHP increases, while mean CP sustains its value from 12h to 36h. Mean MLHP significantly decreases from 12h to 24h due to SSC. After 36h, mean CP rapidly falls again when mean MLHP significantly increases.

Figure 2 depicts the time series of mean central pressures (CPs) and mean latent heat fluxes averaged from 1997 to 2005 in SG and their standard deviations. The variation of mean latent heat flux is similar to that of mean MLHP in the sense that mean latent heat flux is high at the early integration from 6h to 9h and increases after 36h. Therefore, mean CP is closely related to mean MLHP and mean latent heat flux, suggesting that not only sea-surface temperature but also upper ocean sea temperature and salinity are related to Hai-Tang's intensity through the variation of latent heat flux during Hai-Tang's passage. It should be noted that the result is independent of the variation of oceanic precondition.

The impact of the variation of oceanic precondition on latent heat flux is represented by the amplitude of standard deviation. In this study, we address the amplitude of standard deviation in order to investigate the impact of the variation of oceanic preconditions. Figure 3 displays the horizontal distributions of mean latent heat flux in SG (Fig.3a) and NH (Fig.3c) and those of standard deviation in SG (Fig.3b) and NH (Fig.3d). Mean latent heat flux is high west of Hai-Tang's center in SG (Fig.3a). The amplitude of standard deviation is high near Hai-Tang's center in SG (Fig.3b) and NH (Fig.3d) even though the pattern is not similar each other.

Wave-1 asymmetry displayed in Fig. 3a is remarkable due to SSC, while its axisymmetric pattern is emphasized in Fig.3c without SSC effect. Even though the difference of horizontal distribution is salient between SSC (SG) and no SSC (NH), the impact of the variation of oceanic precondition is remarkable near Hai-Tang's center where MLHP is high. The distribution of the standard deviation of latent heat flux may demonstrate the correlation between mean MLHP and mean latent heat flux. It should be noted that the numerical-prediction experiments includes the effect of cumulus parameterization on the results of prediction. We should investigate the impact of the variation of oceanic precondition on TC prediction using cloud-resolving nonhydrostatic atmospheric model without using cumulus parameterization, coupled with the ocean model.

References

Usui, N., S. Ishizaki, Y. Fujii, H. Tsujino, T. Yasuda and M. Kamachi, 2006: Meteorological Research Institute multivariate ocean variational estimation (MOVE) system: Some early results. *J. Adv. Space Res.*, **37**, 806-822.
Wada, A., 2009: Idealized numerical experiments associated with the intensity and rapid intensification of stationary tropical cyclone-like vortex and its relation to initial sea-surface temperature and vortex-induced sea-surface cooling, *J. Geophys. Res.*, **114**, D18111

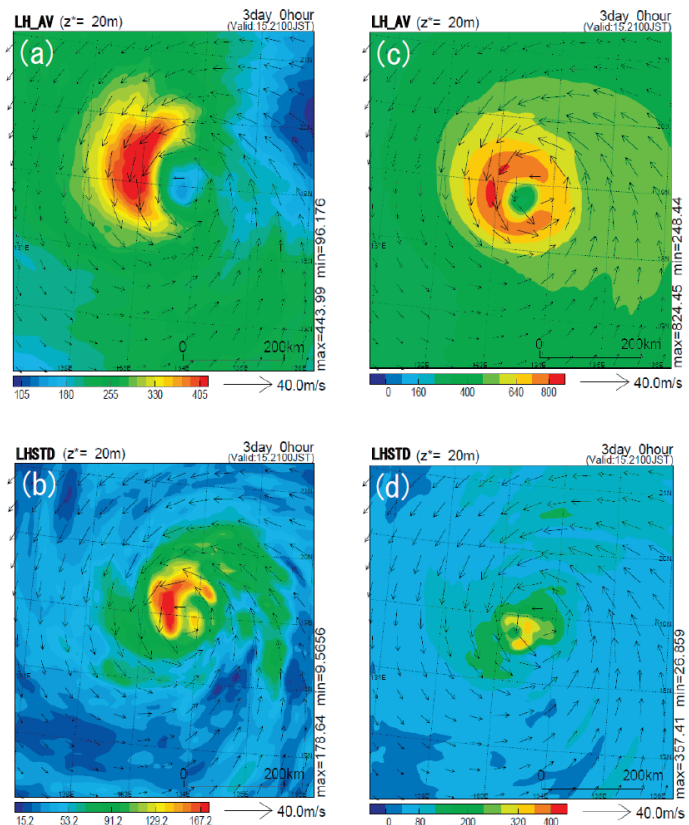


Figure 3 Horizontal distribution of (a) mean latent heat flux and mean surface wind in SG, (b) standard deviation in SG, (c) mean latent heat flux and mean surface wind in NH, and (d) standard deviation in NH at 72h.

Formulation of the effect of breaking surface waves on entrainment and its impact on Typhoon Hai-Tang in 2005

Akiyoshi Wada^{1*}, Nadao Kohno² and Yoshimi Kawai³

1) Meteorological Research Institute, Tsukuba, Ibaraki, 305-0052, JAPAN

2) Japan Meteorological Agency, Chiyoda, Tokyo, 100-8122, JAPAN

3) Japan Agency for Marine-Earth Science and Technology, Yokosuka, Kanagawa, 237-0061, JAPAN

1. Introduction

The most important process associated with TC-ocean interaction is sea-surface cooling (SSC) caused by the passage of a tropical cyclone (TC). SSC plays a role in weakening mesovortices formed on spiral bands within a TC-scale cyclonic circulation during TC intensification phase. The weakened mesovortices leads to the suppression of TC intensification [Wada, 2009]. In addition, the state of ocean waves is closely related to both air-sea momentum and enthalpy transfers through the variation of roughness length. In particular, drag coefficients level off at very high wind speed [e.g., Powell et al., 2003; Donelan et al., 2004]. Here, we address the relationship between the state of ocean waves and SSC. The state of ocean waves possibly affects the formation of SSC through the effect of breaking surface waves. Therefore we need to clarify how breaking surface waves affect the formulation of SSC in an atmosphere-wave-ocean coupled system. In this study, we formulate the effect of breaking surface waves on entrainment under the assumption that breaking surface waves are expressed as a function of wave-induced stress. In addition, we investigate the impact of entrainment induced by breaking surface waves on the ocean response to Typhoon Hai-Tang in 2005. Moreover, we investigate the influence of wave-ocean interaction on Hai-Tang's intensity predicted by the atmosphere (NHM)-wave (MRI-III)-ocean (MLOM) coupled model [Wada et al., 2009]. In this study, central pressure (CP) is used as the reference of best-track intensity.

2. Wave-ocean interaction

Surface currents calculated by the ocean model are provided to the ocean wave model and wave-induced stresses are provided to the ocean model as the ocean-wave coupling procedure between MRI-III and MLOM [Wada et al., 2009]. Wave-induced stresses are calculated by the ocean wave model as follows.

$$\tau_w = \rho_w g \int \frac{S_{in}}{c_p} d\theta d\omega, \quad (1)$$

where τ_w indicated the wave-induced stress, ρ_w is the sea-water density, g is the gravitational acceleration, S_{in} indicates the wind-input source term in the action balance equation, and c_p is the phase velocity at the peak of the spectrum. θ is the wave direction and ω is the wave frequency. The parameter m_d for breaking surface waves induced by wind stress [Wada et al., 2009] is calculated under the assumption that the effect of breaking surface waves is expressed as a function of wave-induced stress and surface wind stress.

$$m_d = c_{wm} \frac{\tau_w}{\tau} \Delta t, \quad (2)$$

where τ indicates the surface wind stress and Δt is the time step of the ocean model. C_{wm} is the constant value and is assumed to be 2. Surface wind speed and surface wind stresses calculated in the atmosphere model are provided to the ocean wave model. Roughness lengths is calculated by the wave steepness [Taylor and Yelland, 2001], which is calculated in the ocean wave model.

3. Experiment Design

Table 1 lists four numerical experiments for investigating the sensitivity of breaking surface waves to SSC and Hai-Tang's prediction during its intensification phase. The initial integration time is 1200 UTC 12 July in 2005. At the beginning, three runs are performed using the atmosphere-wave-ocean coupled model [Wada et al., 2009] with a horizontal grid spacing of 3km. The abbreviations mean only atmosphere model (A3), atmosphere-ocean coupled model (AO3) and atmosphere-wave-ocean model (AWO3). In addition, another run is performed using the same atmosphere-wave-ocean coupled model except for $m_d=175$ (AWO3C).

The specification in the atmosphere model for the present numerical-prediction experiments is as follows. The number of horizontal grid is 1441 x 841 with a horizontal grid spacing of 3 km. The number of vertical

level is 40 at which the interval is variably stretched from 40 m at the lowest layer near the surface and 1180 m at the uppermost layer. The top height is nearly 23 km. The specification for atmospheric initial and boundary conditions and oceanic initial conditions are described in Wada et al. [2009].

Table 1 Abbreviation of Each Numerical Experiment, Horizontal Resolution, and Model Speculation

Experiment	Horizontal resolution (km)	Model
A3	3km	NHM
AO3	3km	NHM + MLOM
AWO3	3km	NHM+MRI-III+MLOM & Eq.(3)
AWO3C	3km	NHM+MRI-III+MLOM & $m_d=1.75$

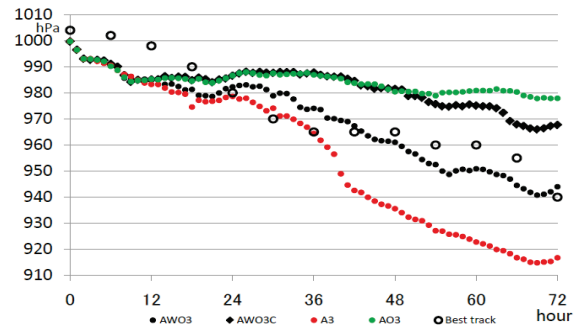


Fig. 1 Time series of Hai-Tang's best-track central pressure every six hours and hourly predicted central pressures in A3, AO3, AWO3, and AWO3C.

4. Results

Figure 1 depicts the time series of best-track CPs, archived by the Regional Specialized Meteorological Center, every six hours and its hourly predicted CPs from 1200 UTC on 12 July (0h) to 1200 UTC on 15 July (72h). At the early integration, hourly predicted CPs indicate rapid intensification, while a change in best-track CPs is small compared with the change in hourly predicted CPs. After 9h, a difference in hourly predicted CPs become significant between A3, AO3, and AWO3. From 15h to 24h, Hai-Tang's intensification is suppressed due to SSC.

After 24h, a trend in hourly predicted CPs in AO3 turns to differ from the trends in A3 and AWO3 and similar to the trend in AWO3C. The impact of a difference in the specifications between AO3 and AWO3C on predicted CP becomes significant after 48h. In contrast, a difference in predicted CPs between AWO3 and AWO3C becomes significant at 15h. The difference occurs earlier than that in predicted CPs between AO3 and AWO3C. This suggests that the parameter m_d plays an important role in predicting Hai-Tang's intensity.

At 72h, predicted CPs in A3 are extremely lower than the best-track CPs, while those in AO3 are higher than the best-track CPs. Even though predicted Hai-Tang excessively develops after 42h in AWO3, predicted CPs are rather comparable to the best-track CPs than the other predicted CPs (Fig. 1). Therefore, the introduction of Eq. (2), for calculating the effect of breaking surface waves on entrainment using wave-induced stress calculated in the ocean wave model, leads to the improvement of Hai-Tang's intensity prediction in that Hai-Tang's intensification in AWO3 is better reproduced than that in AWO3C.

Figure 2 displays the horizontal distribution of initial mixed-layer depth and SSC at 72h. SSC is enhanced around Hai-Tang's center and on the right side of predicted Hai-Tang's track. SSC saliently occurs where initial mixed-layer depth is relatively shallow (Red circle in Fig. 2). This suggests that SSC is controlled not only by Hai-Tang's intensity but also the variation of pre-existing oceanic condition, particularly the distribution of mixed-layer depth.

It should be noted that we can use Eq. (2) only when the atmosphere-wave-ocean coupled model is used. We may need another formulation without coupling the ocean wave model because the computational cost for running the ocean wave model is expensive.

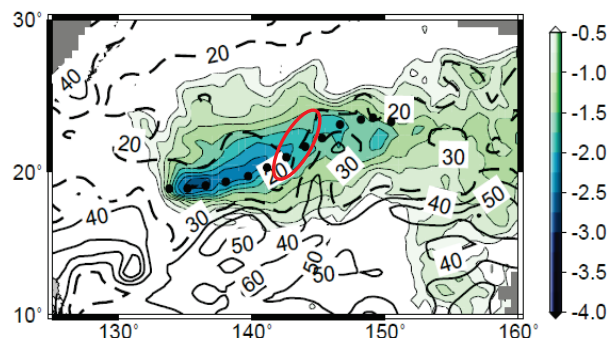


Fig. 2 Contours indicate horizontal distributions of initial mixed-layer depth (solid lines indicate depths more than 40m and dashed lines indicate depths less than 30m) at 1200 UTC on 12 July (upper panel) and shading indicates SSC at 72h from the initial time.

References

- Donelan, M. A., B. K. Haus, N. Reul, W. J. Plant, M. Stiassnie, H. C. Graber, O. B. Brown, and E. S. Saltzman, 2004: On the limiting aerodynamic roughness of the ocean in very high winds, *Geophys. Res. Lett.*, 31, L18306.
- Powell, M. D., P. J. Vickery, and T. A. Reinhold, 2003: Reduced drag coefficient for high wind speeds in tropical cyclones, *Nature*, 422, 279-283.
- Wada, A., 2009: Idealized numerical experiments associated with the intensity and rapid intensification of stationary tropical cyclone-like vortex and its relation to initial sea-surface temperature and vortex-induced sea-surface cooling, *J. Geophys. Res.*, 114, D18111.
- Wada, A., N. Kohno and N. Usui, 2009: Numerical predictions for Typhoon Hai-Tang in 2005 by an experimental atmosphere-wave-ocean coupled model. *CAS/JSC WGNE Res. Activ. Atmos. Oceanic Modell.* 0911-0912.

This work was supported by Japan Society for the Promotion of Science (JSPS), Grant-in-Aid for Scientific Research (C) (19612005).